Mechanisms and Dynamics of Protein Clustering on a Solid Surface

P. A. Mulheran,[1] D. Pellenc,[2] R. A. Bennett,[2] R. J. Green,[3] and M. Sperrin[4]

[1]*Department of Chemical and Process Engineering, University of Strathclyde, James Weir Building, 75 Montrose Street, Glasgow G1 1XJ, United Kingdom*

[2]*Department of Physics, University of Reading, Whiteknights, Reading RG6 6AF, United Kingdom*

[3]*School of Pharmacy, University of Reading, Whiteknights, Reading RG6 6AF, United Kingdom*

[4]*Medical Physics and Clinical Engineering, Royal Berkshire Hospital, London Road, Reading RG1 5AN, United Kingdom*

(Received 13 February 2007; published 12 February 2008)

A methodology for discovering the mechanisms and dynamics of protein clustering on solid surfaces is presented. *In situ* atomic force microscopy images are quantitatively compared to Monte Carlo simulations using cluster statistics to differentiate various models. We study lysozyme adsorption on mica as a model system and find that all surface-supported clusters are mobile, not just the monomers, with diffusion constant inversely related to cluster size. The surface monomer diffusion constant is measured to be $D_1 \sim 9 \times 10^{-16}$ cm^2 s^{-1}, such a low value being difficult to measure using other techniques.

DOI: 10.1103/PhysRevLett.100.068102 PACS numbers: 87.85.J−, 87.14.E−, 87.16.A−, 68.43.Jk

Protein binding onto solid surfaces is a key process in many biotechnological systems [1], from the design of biosensors to the biocompatibility of implants [2]. The conformation of the proteins on a substrate is crucial for their activity [3]. The arrangement of the proteins across the substrate deserves particular attention, since it provides mesoscale morphology for interactions with tissue [4] and also influences conformation [5]. If we understand the mechanisms by which proteins cluster together on the surface, we might hope to influence the growth of the protein layers and hence engineer bioactive surfaces with tailored properties.

Surprisingly, the mechanisms and dynamics of protein aggregation on solid substrates has not been studied in much detail prior to this Letter. Random sequential adsorption (RSA) models are widely assumed to be adequate, whereby surface diffusion is at best limited to cluster rearrangements with no long-range center-of-mass diffusion [6]. However atomic force microscopy (AFM) images repeatedly show clustering of proteins, which indicate that such models are inadequate [7–9]. In contradiction, the kinetics of protein adsorption are often modeled using Langmuir kinetics, where it is implicitly assumed that in late stage adsorption the proteins have clustered so that all the free surface is available for further adsorption rather than being ''jammed'' as in the RSA models [10]. While some authors have attempted to account for surface diffusion and lateral interactions in protein adsorption models [11,12], detailed comparisons to experimental data are lacking. Furthermore, a methodology to enable a quantitative understanding of both the mechanisms and the rates of diffusion and clustering on a solid substrate has not been established for this field until now.

In this Letter we shall adopt the powerful methodology used in island nucleation and growth studies of condensed matter systems, where growth mechanisms and relevant diffusion rates have been quantified using the statistical properties of grown island arrays [13,14]. We study lysozyme (a small, robust globular protein) clustering on mica, followed *in situ* by AFM, and use statistical analysis of the images to make quantitative comparisons to Monte Carlo simulations. Surprisingly, we find that the lysozyme clusters are significantly mobile on the substrate, a result quite at odds with any previous quantitative model for protein adsorption at a solid surface.

Figure 1 shows typical *in situ* images of the lysozyme clusters taken after different exposure times using tapping-mode AFM. The lysozyme (L6876, Sigma-Aldrich) is deposited onto freshly cleaved mica from a 3 mm depth of solution under stagnant conditions, at a concentration of 1 μg/mL in *p*H4/ionic strength 0.02 M buffer at 22 °C. The saturation fractional substrate coverage is estimated to be 0.36 (see below). We performed tests to establish that imaging did not influence the adsorption of the protein and the areas shown are representative of the patterns we repeatedly observed under these and similar conditions. We have also compared images from supersharp and normal tips and conclude that tip-convolution effects are not important in this study. One key feature of these images is that the clusters always remain at one protein height, and we obtain no evidence for multilayer growth, in agreement with previous reports [7].

In Fig. 2 we show how the surface coverage by the lysozyme monotonically increases over time as expected for irreversible adsorption [7]. Furthermore, its variation is consistent with solutions of the diffusion equation, using the uncovered substrate as an adsorbing boundary as in classic Langmuir kinetics. We find the bulk diffusion constant, D_b, of the lysozyme in the solution $\sim 10^{-6}$ cm^2 s^{-1}, consistent with the literature values for this *p*H and ionicity [15]. In Fig. 2 we also show how the coverage dependence is affected by the adsorption probability onto the bare substrate. Not all adsorption attempts are necessarily successful as the correct orientation of the protein is expected

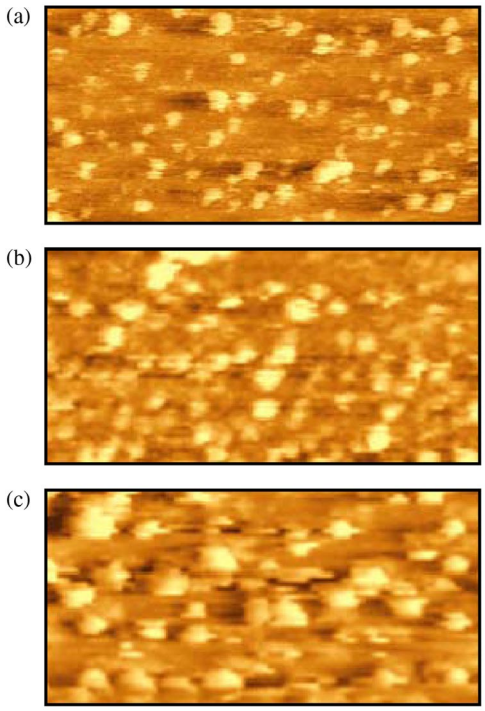

FIG. 1 (color online). AFM images (500 nm × 250 nm) of protein clusters after different exposure times: (a) 74 000 s; (b) 100 000 s; (c) 182 000 s. The images are not from the same area but are representative of those taken across the substrate at the times shown.

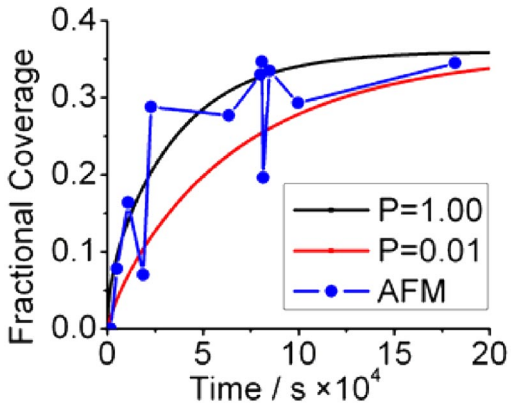

FIG. 2 (color online). Coverage of the substrate observed in the AFM experiments against exposure time. The smooth curves come from a solution of the diffusion equation, assuming translational symmetry across the system, starting with a uniform distribution of the lysozyme in solution and a bare adsorbing substrate. The sticking coefficient onto bare substrate is $P = 1.0$ and $P = 0.01$.

to be crucial for its adsorption [16]. In the work that follows we shall assume that this probability of adsorption is $P = 0.01$.

To determine the mechanisms and rates of the cluster growth, we investigate a range of Monte Carlo simulations. We start with an RSA model where proteins are deposited at random onto bare substrate at the time-dependent rate determined from Fig. 2. The substrate is represented by a square mesh with lattice spacing of 3 nm to match the size of the lysozyme. Sites are occupied by single monomers that do not diffuse, but they can hop to nearest and next-nearest sites within a given cluster to increase the internal connectivity. Figure 3(a) shows typical protein arrangements predicted by this model after 100 000 s. As expected, this RSA model produces very different patterns to those observed. It is unlikely that direct adsorption from solution at the edge of existing clusters is strongly preferred over adsorption at the bare mica due to the negative charge carried by the mica at this pH and the positive charge on the lysozyme, and certainly no multilayer growth is observed. We conclude that surface diffusion must be important for the clustering [7].

We now include monomer surface diffusion in our models by allowing free monomers to hop to nearest sites at a rate ν. First we consider the behavior for critical cluster size $i = 1$ whereby diffusing monomers must come together to nucleate a stable, immobile cluster [13,14]. Figure 3(b) shows typical cluster arrays grown in this simulation where the surface diffusion constant of the monomers $D_1 = 9 \times 10^{-14}$ cm^2 s^{-1}. The cluster array has a degree of regularity in its spatial arrangement, and in its range of cluster sizes and shapes, which can be understood in terms of cluster growth inside capture zones for deposited monomers. These are the Voronoi-type edge cells also shown in Fig. 3(b); each zone marks the region of the substrate closer to the adsorbing edge of the resident cluster than to any other cluster edge [17,18].

The positions of the clusters in the $i = 1$ model are determined by the stochastic nucleation events that can continue through the adsorption process. An alternative model can be made by considering only growth from predetermined seeds, possibly pinned to undetected substrate defect sites, thereby establishing unchanging capture zones at the start of growth [19]. While we do not show results of this variation here, the statistics of this model are briefly discussed below.

Next we turn to a similar model but with critical cluster size $i = 0$ so a diffusing monomer can spontaneously nucleate a cluster, perhaps following a conformational change. The image in Fig. 3(c) has been created with the probability 10^{-4} per monomer hop of spontaneous nucleation, with $i > 0$ nucleation suppressed. This image supports a more favorable comparison to the AFM data, although there does appear to be more coalescence of the clusters in the experiment.

We turn now to our final variation of the simulation, where all clusters are mobile but with a size-dependent diffusion constant $D_s = D_1/s$ which varies inversely with cluster size s (measured in monomers). The clusters diffuse rigidly without rotation by moving their center-of-mass by one nearest neighbor lattice spacing [20]. This mechanism allows for more cluster coalescence as seen in Fig. 3(d),

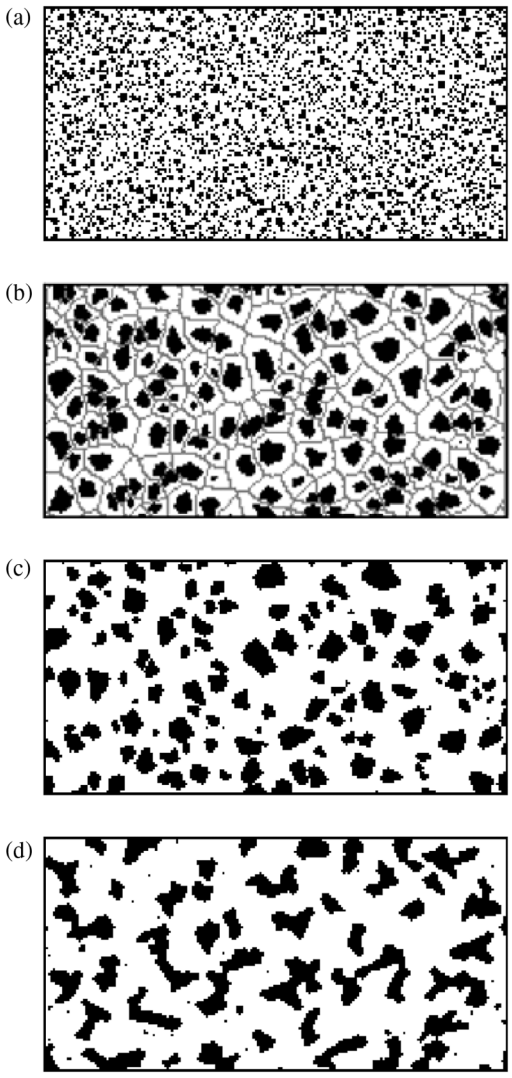

FIG. 3. Comparison of simulated cluster arrays at 100 000 s: (a) An RSA model with attractive interaction between monomers; (b) Cluster nucleation and growth model for critical cluster size $i = 1$ with Voronoi-type edge cells superposed in gray; (c) Cluster nucleation and growth model with $i = 0$; (d) Model with mobile clusters.

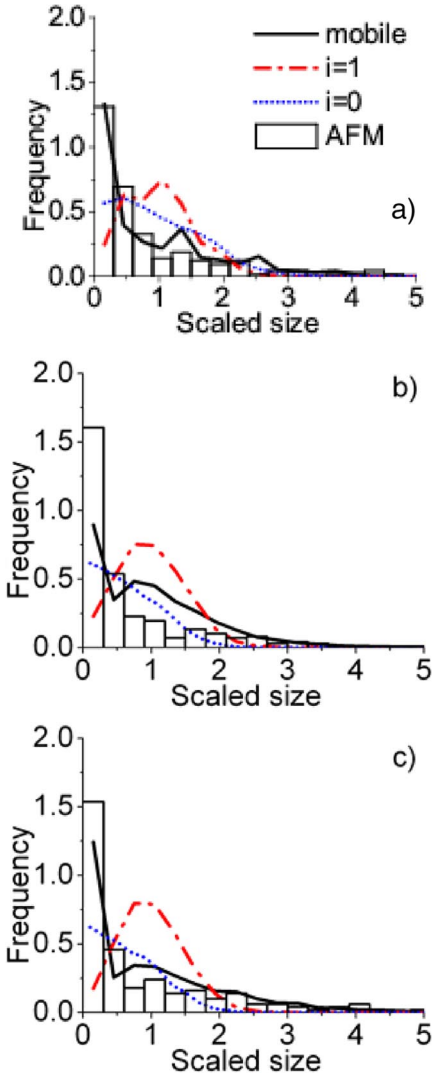

FIG. 4 (color online). Cluster size distributions at time (a) 10 000 s; (b) 80 000 s; (c) 180 000 s. The abscissa are scaled to the mean size at each time. The bars are from the AFM experiments and the lines from the simulations with mobile clusters, and with critical cluster sizes $i = 1$ and $i = 0$. Pearson's correlations have been calculated for each model distribution in comparison to the AFM data, and in the order of mobile clusters, $i = 1$ and $i = 0$ are (a) 0.96, 0.42, 0.85; (b) 0.86, 0.25, 0.80; (c) 0.97, 0.20, 0.79.

where $D_1 = 9 \times 10^{-16}$ cm^2 s^{-1}, and a consequently better visual comparison with AFM images.

In order to quantify the comparison between the models and the AFM images, we examine the cluster size distributions [13,14]. In Fig. 4 we show the size distributions from AFM images at various times, alongside those from $i = 0$, $i = 1$, and mobile cluster simulations. The $i = 1$ distributions follow a singly peaked distribution that is slightly broader than that of the capture zones due to the nucleation of new clusters as growth proceeds [17]. For growth solely from defect sites the cluster sizes will exactly mirror the unchanging distribution of capture zones for the defects, again yielding a singly peaked distribution [19]. In contrast, the $i = 0$ distributions display a monotonically decreasing form due to the broadening caused by significant cluster nucleation throughout the growth [21]. The size distributions from the mobile cluster simulations are broader still [22] as the mobility disrupts the capture zones.

The AFM size distributions are in contrast to those of $i = 0$, 1, particularly at later times in Figs. 4(b) and 4(c). Here the characteristic trends in the data become more apparent and follow more faithfully those of the mobile cluster simulations. The Pearson's correlation values given in the figure caption confirm this, indicating that the mobile cluster model best represents the mechanisms at play.

A key signature of the cluster mobility is that the cluster number density should fall at later times when coalescence

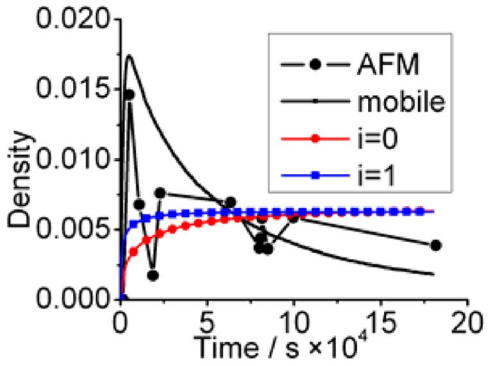

FIG. 5 (color online). Cluster density (number per 3 nm × 3 nm area) evolution over time from AFM images and the simulation models.

outweighs deposition [20]. In Fig. 5 we show that this is precisely what is observed in our AFM images and the mobile cluster simulation. In neither case is the early peak in cluster density due solely to monomers, and, therefore, could not be accounted for in either of the critical cluster size models or by growth from substrate defects.

We have also considered mobile cluster simulations with diffusion constant $D_s = D_1 s^{-\mu}$ where the mobility parameter μ is changed to reflect different diffusion mechanisms [23]. With $\mu = 1.5$, expected when protein hopping around the edge of the cluster induces the center-of-mass diffusion, the cluster size distributions become too peaked at later times, similar to the $i = 1$ distributions in Fig. 4. With $\mu = 0.5$, expected when monomer evaporation and condensation within a reservoir of surface monomers dominates the cluster mobility, the simulation can yield competitive size distributions using the protein adsorption coefficient $P = 1$. However, we now find that the cluster density is extremely low at long times regardless of the monomer diffusion coefficient D_1, because the large clusters retain high mobility. Details of these models will be presented elsewhere. We conclude that the model we present here with $P = 0.01$ and $\mu = 1$, possibly indicating monomer diffusion over the protein cluster as a dominant mechanism for cluster mobility, provides the best quantitative comparison with the AFM data.

This model provides an estimate for the lysozyme monomer surface diffusion rate through the fit to the cluster density data of Fig. 5, which can be achieved without significantly changing the scaled cluster size distributions of Fig. 4. The result is $D_1 \sim 9 \times 10^{-16}$ cm^2 s^{-1}, such a low value being very difficult to obtain from other techniques. We found only one paper attempting to quantify the rate of lysozyme diffusion across a mica surface, estimating the single protein (monomer) diffusion rate $D_1 \sim 10^{-16}$ cm^2 s^{-1} from a rudimentary consideration of the length and time scales of the clustering observed in AFM images [7].

In summary, we have provided a quantitative analysis of the clustering mechanisms observed in AFM images of lysozyme deposition onto mica. We show conclusive evidence for mobility of not just protein monomers but also of protein aggregates. The work demonstrates the pitfalls of assuming that the adsorption follows a simple RSA model, and shows that intuitive assumptions about diffusion and nucleation mechanisms can be misleading.

This work was funded by an MRC/BBSRC/EPSRC Discipline Hopping Grant No. G0401479 and supported by the Royal Society/Wolfson Foundation through laboratory refurbishment.

[1] J. J. Gray, Curr. Opin. Struct. Biol. **14**, 110 (2004).
[2] B. Kasemo, Surf. Sci. **500**, 656 (2002).
[3] S. S. Karajanagi, A. A. Vertegel, R. S. Kane, and J. S. Dordick, Langmuir **20**, 11594 (2004).
[4] B. R. Smith, H. M. Rinder, and C. S. Rinder in *Thrombosis and Hemorrage*, edited by J. Loscalzo and A. I. Schafer (Williams and Wilkins, Baltimore, 2003), 3rd ed.
[5] P. Y. Meadows, J. E. Bemis, and G. C. Walker, Langmuir **19**, 9566 (2003).
[6] J. Talbot, G. Tarjus, P. R. Van Tassel, and P. Viot, Colloids Surf. A **165**, 287 (2000).
[7] D. T. Kim, H. W. Blanch, and C. J. Radke, Langmuir **18**, 5841 (2002).
[8] T. J. McMaster, M. J. Miles, P. R. Shewry, and A. S. Tatham, Langmuir **16**, 1463 (2000).
[9] D. C. Cullen and C. R. Lowe, J. Colloid Interface Sci. **166**, 102 (1994).
[10] J. J. Ramsden, G. I. Bachmanova, and A. I. Archakov, Phys. Rev. E **50**, 5072 (1994).
[11] A. P. Minton, Biophys. J. **80**, 1641 (2001).
[12] S. Ravichandran and J. Talbot, Biophys. J. **78**, 110 (2000).
[13] J. W. Evans, P. A. Thiel, and M. C. Bartelt, Surf. Sci. Rep. **61**, 1 (2006).
[14] H. Brune, Surf. Sci. Rep. **31**, 125 (1998).
[15] S. B. Dubin, A. C. Noel, and G. B. Benedek, J. Chem. Phys. **54**, 5158 (1971).
[16] S. Ravichandran, J. D. Madura, and J. Talbot, J. Phys. Chem. B **105**, 3610 (2001).
[17] P. A. Mulheran and J. A. Blackman, Phys. Rev. B **53**, 10261 (1996).
[18] M. C. Bartelt, A. K. Schmid, J. W. Evans, and R. Q. Hwang, Phys. Rev. Lett. **81**, 1901 (1998).
[19] P. A. Mulheran and J. A. Blackman, Philos. Mag. Lett. **72**, 55 (1995).
[20] P. A. Mulheran and D. A. Robbie, Phys. Rev. B **64**, 115402 (2001).
[21] P. A. Mulheran and D. A. Robbie, Europhys. Lett. **49**, 617 (2000).
[22] P. L. Krapivsky, J. F. F. Mendes, and S. Redner, Phys. Rev. B **59**, 15950 (1999).
[23] S. V. Khare, N. C. Bartelt, and T. L. Einstein, Phys. Rev. Lett. **75**, 2148 (1995).